Quantitative Optical Coherence Tomography Analysis for Late In-Stent Restenotic Lesions

Qiang Fu,[1,2] MD, Nobuaki Suzuki,[1] MD, Ken Kozuma,[1] MD, Mutsuki Miyagawa,[1] MD, Takahiro Nomura,[1] MD, Hideyuki Kawashima,[1] MD, Yoshitaka Shiratori,[1] MD, Shuichi Ishikawa,[1] MD, Hiroyuki Kyono,[1] MD, *and* Takaaki Isshiki,[1] MD

Summary

Coronary optical coherence tomography (OCT) has the potential to identify in-stent neoatherosclerosis, which is a possible risk factor for late acute coronary events after drug-eluting stent implantation. The purpose of this study was to investigate differences between mid-term and late in-stent restenosis after stent implantation by quantitative and semiautomated tissue property analysis using OCT. In total, 1063 OCT image frames of 16 lesions in 15 patients were analyzed. This included 346 frames of 6 lesions in late in-stent restenosis, which was defined as restenosis that was not detected at 6 to 12 months but ≥ 12 months after follow-up coronary angiography. Signal attenuation was circumferentially analyzed using a dedicated semiautomated software. Attenuation was assessed along 200 lines delineated radially for analysis of the in-stent restenotic lesions (between the lumen and stent contours). All lines were anchored by the image wire to avoid artifacts resulting from wire location. Stronger signal attenuation at the frame level (2.46 ± 0.78 versus 1.47 ± 0.32, $P < 0.001$) and higher maximum signal intensity at the lesion level (9.19 ± 0.19 versus 8.84 ± 0.32, $P = 0.018$) were observed in late in-stent restenotic lesions than in mid-term in-stent restenotic lesions. OCT demonstrated stronger signal attenuation and higher maximum signal intensity in late in-stent restenotic lesions than in mid-term in-stent restenotic lesions, indicating the possibility of neoatherosclerosis. (Int Heart J 2015; 56: 13-17)

Key words: Coronary artery disease, Intracoronary imaging, Restenosis, Percutaneous coronary intervention

Drug-eluting stent (DES) placement decreases the incidence of mid-term in-stent restenosis.[1)] However, late in-stent restenosis is occasionally observed in cases of previous DES implantation.[2)] Thrombus formation or inflammatory cell proliferation in late in-stent restenotic lesions after DES implantation may indicate a delayed healing process.[3)] Coronary optical coherence tomography (OCT) has emerged as an effective modality to elucidate the healing process after stent implantation.[4-8)] Strong signal attenuation is commonly observed in late in-stent restenotic lesions on OCT.[9)] One recent study revealed the utility of OCT combined with virtual histology intravascular ultrasound in identifying neoatherosclerosis in late in-stent restenosis after DES implantation.[10)] Strong signal attenuation on OCT may indicate neoatherosclerosis.[4,11)] In addition, macrophage proliferation is indicated by high signal intensity on OCT images.[12)] Quantitative evaluation of signal attenuation and intensity may enable identification of neoatherosclerosis after DES implantation. In the present study, we analyzed OCT signal intensity and attenuation for tissue property analysis of in-stent restenotic lesions using a contemporary quantitative analysis system. The purpose of this study was to investigate differences between mid-term and late in-stent restenosis by using a quantitative OCT analysis system.

Methods

Intracoronary OCT images from patients with in-stent restenosis after stent implantation were evaluated retrospectively. Sixteen in-stent restenotic lesions from 15 patients were analyzed in 1063 frames showing stenosis of > 50% on OCT. Cases of late in-stent restenosis were defined as those not identified at 6 to 12 months but ≥ 12 months after follow-up coronary angiography and those requiring percutaneous coronary intervention. Observers were blinded to patient demographics during the quantitative image analysis.

This study was approved by the ethics committee of our institution. Because of its retrospective nature, informed consent was waived for this study according to Japanese standard ethical policy established by the Ministry of Health, Labor and Welfare.

Image acquisition: The OCT system used in the present study included a computer, a display monitor, an interface unit (M3x Cardiology Imaging System, LightLab Imaging, Inc., Westford, MA, USA), and a 0.019-inch imaging wire (ImageWire,

From the [1] Department of Medicine, Teikyo University School of Medicine, Tokyo, Japan and [2] Department of Cardiology, Beijing Tiantan Hospital, Capital Medical University, Beijing, China.

Address for Correspondence: Nobuaki Suzuki, MD, Department of Medicine, Teikyo University School of Medicine, 2-11-1 Kaga, Itabashi-ku, 173-8606 Tokyo, Japan. E-mail: nsuzu@bronze.ocn.ne.jp

Received for publication April 29, 2014. Revised and accepted June 9, 2014.

Released in advance online on J-STAGE December 11, 2014.

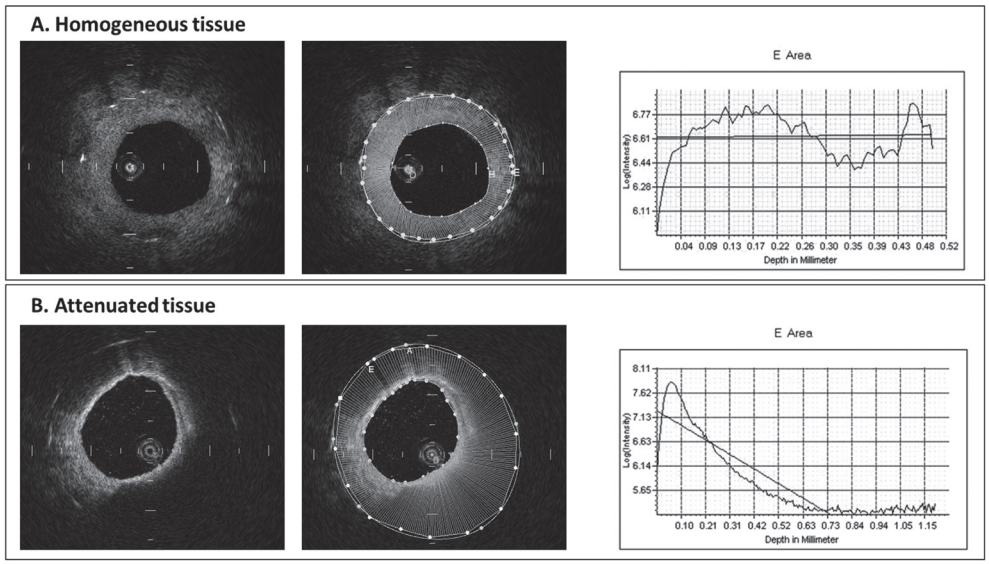

Figure 1. Representative image showing homogeneous (**A**) and attenuated lesions (**B**).

LightLab Imaging). Images were acquired during automatic pullback at 1 mm/s and 20 frames/s. Prior to the procedure, 100 IU/kg of heparin was administered. The OCT image system was introduced into the target coronary artery segment through a 6-Fr or 7-Fr guiding catheter. A dedicated occlusion balloon catheter (Helios, Avantec Vascular Corp., Sunnyvale, CA, USA) was inflated up to 0.7 atm proximal to the target segment. During inflation, the distal part of the vessel was flushed with heparinized Ringer's lactate to clear it of blood and ensure optimal image quality.

OCT image analysis: All cross-sectional images (frames) were initially screened for quality assessment. Frames were excluded from the analysis if stent struts were not visible on the screen, a side branch ostium occupied > 45° of the target vessel lumen, or residual blood was mistaken for neointimal tissue. Sew-up artifacts (image misalignment resulting from rapid movement of the artery or transducer during the capture of a single frame)[4] or reverberations that interfered with objective analysis were also excluded.[13] Measurements on OCT cross-sectional images were obtained using a dedicated automated contour detection system (OCT system software, LightLab Imaging). The lumen contour was delineated automatically. Stent struts were positioned manually in the center of the stent strut which showed a bright "blooming" appearance.[14] The contour of the stent area was delineated by connecting the stent struts. Both contours were delineated with cubic spline interpolation. The wire–lumen line was delineated as a line with the minimal distance from the lumen to the image wire. A wire concentric index (WCI) was created as a scale of eccentricity of the wire location inside of the lumen, and was calculated as the distance of the wire-lumen line divided by lumen radius: WCI = wire-lumen distance/lumen radius. Automatic signal attenuation analysis was performed circumferentially between the lumen and stent contours.[15] Attenuation was assessed along 200 lines for the in-stent restenotic tissue. All lines were anchored by the image wire to avoid artifacts resulting from wire location. Theoretically, the influence of refraction and focusing of the beam on signal attenuation should be minimal in this direction. Signal level was plotted on a graph with the x-axis representing depth (mm) and the y-axis representing signal intensity value (natural log scale). Maximum signal intensity was evaluated for the total neointimal area. Representative frames showing homogeneous and attenuated lesions are presented in Figure 1.

Interobserver and intraobserver variability: Two independent observers (NS and FQ) analyzed the best 50 cross-sectional images without artifacts. Measurements were performed by both observers at the first time point, and the measurements were repeated by 1 of the observers after 1 month. Interobserver and intraobserver agreement was determined by calculating values for differences in measurements of lumen and stent area, extent of in-stent restenosis, maximum signal intensity, and signal attenuation.

Statistical analysis: Continuous values are expressed as the mean ± standard deviation and were compared using an unpaired *t*-test. Correlations were analyzed by a linear regression test. Agreement between the 2 observers (interobserver variability) was investigated using a paired *t*-test and linear regression analysis. For the results of the unpaired *t*-test, differences were considered statistically significant at $P < 0.05$. Statistical analyses were performed using JMP software (SAS Institute, Cary, NC, USA).

Results

Table I shows the variability and correlations for each parameter between the 2 observers and observation points. Acceptable levels of agreement and correlation were observed.

Table II displays the characteristics of the patients and lesions. Late in-stent restenosis was identified in 346 frames of 6 (38%) lesions. Nine (56%) lesions showed in-stent restenosis after DES implantation. Primary coronary artery disease was identified as acute coronary syndrome in 4 (25%) lesions. There were no complications related to the OCT procedure.

Lesion-level data: Table III shows the differences between pa-

Table I. Intraobserver and Interobserver Variability

	Agreement					Correlation			
	Observer 1	Observer 1'	Observer 2	P: Observer 1 versus 1'	P: Observer 1 versus 2	r: Observer 1 versus 1'	P: Observer 1 versus 1'	r: Observer 1 versus 2	P: Observer 1 versus 2
Lumen area (mm^2)	1.88 ± 1.31	1.88 ± 1.30	1.89 ± 1.32	0.28	0.25	1	< 0.001	1	< 0.001
Stent area (mm^2)	5.22 ± 2.29	5.24 ± 2.27	5.17 ± 2.38	0.61	0.08	1	< 0.001	1	< 0.001
Stenotic area (%)	66.2 ± 12.2	66.5 ± 11.8	64.2 ± 14.8	0.15	0.21	0.99	< 0.001	0.68	< 0.001
Maximum signal intensity	8.41 ± 0.28	8.39 ± 0.29	8.41 ± 0.29	0.06	0.41	0.96	< 0.001	0.91	< 0.001
Signal attenuation	1.84 ± 1.01	1.88 ± 1.02	1.84 ± 0.98	0.19	0.91	0.98	< 0.001	0.99	< 0.001

Observer 1: Results of analysis from the first observer at time point 1. Observer 1': Results of analysis from the same observer at time point 2. Observer 2: Results of analysis from the second observer at time point 1.

Table II. Patient and Lesion Characteristics

Variable	
Patient characteristics (n = 15)	
Male (%)	13 (87)
Age (years)	67.7 ± 9.9
Hemodialysis (%)	4 (27)
Diabetes (%)	8 (53)
Hypertension (%)	13 (87)
Dyslipidemia (%)	13 (87)
Smoking history (%)	8 (53)
Lesion characteristics (n = 16)	
Post DES implantation (%)	9 (56)
Late (≥ 12 months) in-stent restenosis (%)	6 (38)
Post ACS (%)	4 (25)
Culprit vessel (%)	
RCA	6 (38)
LAD	7 (43)
LCx	3 (19)

DES indicates drug-eluting stents; ACS, acute coronary syndrome; RCA, right coronary artery; LAD, left anterior descending coronary artery; and LCx, left circumflex coronary artery.

Table III. Differences Between Patients With Mid-Term and Late In-Stent Restenosis

	< 12 months ISR (n = 9)	≥ 12 month ISR (n = 6)	P
Patient characteristics (n = 15)			
Male (%)	8 (89)	5 (83)	1
Age, years	65.2 ± 5.4	66.2 ± 9.7	0.81
Hemodialysis (%)	3 (33)	1 (17)	0.6
Diabetes (%)	5 (56)	3 (50)	1
Hypertension (%)	7 (78)	6 (100)	0.49
Dyslipidemia (%)	8 (89)	5 (83)	1
Smoking history (%)	4 (44)	4 (67)	0.61
Lesion characteristics (n = 16)			
Post DES implantation (%)	6 (60)	3 (50)	1
Chronic total occlusion (%)	0 (0)	1 (17)	0.38
Post-ACS (%)	3 (30)	1 (17)	1
Culprit vessel (%)			0.93
RCA	4 (40)	2 (33)	
LAD	4 (40)	3 (50)	
LCx	2 (20)	1 (17)	
OCT measurement			
Area stenosis, %	71.9 ± 9.3	66.8 ± 12.9	0.37
Lumen area, mm^2	1.74 ± 1.03	2.08 ± 0.64	0.49
Stent area, mm^2	6.23 ± 2.73	6.58 ± 1.28	0.77

DES indicates drug-eluting stents; ACS, acute coronary syndrome; RCA, right coronary artery; LAD, left anterior descending coronary artery; LCx, left circumflex coronary artery; and ISR, in-stent restenosis.

tients with mid-term and late in-stent restenosis. OCT measurements were assessed for the frame revealing maximum area stenosis at each lesion. No significant differences in patient and lesion characteristics were observed between patients with late and mid-term in-stent restenosis. Figure 2A and 2B show the correlation of the wire concentric index (WCI) with the maximum signal intensity and signal attenuation of in-stent restenotic lesions. No correlations were observed between WCI and maximum signal intensity (r = 0.17, P = 0.53) or signal attenuation (r = 0.02, P = 0.94). Figure 2C and 2D present the differences in maximum signal intensity and signal attenuation between mid-term and late in-stent restenotic lesions. Maximum signal intensity was significantly higher in late in-stent restenotic lesions than in mid-term in-stent restenotic lesions (9.19 ± 0.19 versus 8.84 ± 0.32, P = 0.018). Signal attenuation was significantly stronger in late in-stent restenotic lesions than in mid-term in-stent restenotic lesions (2.04 ± 0.31 versus 1.51 ± 0.24, P = 0.01).

Frame-level data: Figure 3A and 3B show very weak correlations of WCI with maximum signal intensity (r = 0.33, P < 0.001) and signal attenuation (r = 0.1, P < 0.001) in in-stent restenotic lesions. Figure 3C and 3D present differences in maximum signal intensity and signal attenuation between mid-term and late in-stent restenotic lesions. Maximum signal intensity was significantly higher (9.14 ± 0.30 versus 8.77 ± 0.43, P < 0.001) and signal attenuation was significantly stronger (2.46 ± 0.78 versus 1.47 ± 0.58, P < 0.001) in late in-stent restenotic lesions than in mid-term in-stent restenotic lesions.

Discussion

The results of the present study suggest that higher maximum signal intensity and stronger signal attenuation can be observed on OCT images in cases of late in-stent restenosis. Neoatherosclerosis may be indicated by these findings, although we still need validation with pathological evidence. Kang, *et al* demonstrated that neoatherosclerosis appears in in-stent restenotic lesions identified > 1 year after DES implantation by showing tissue characterization of in-stent restenosis using OCT imaging.[10] They stated that lipidic intima was defined as a signal-poor region with diffuse borders,[10] which is consistent with the strong signal attenuation caused by relatively high surface signals and lower signals in deeper layers of lesions observed in the current study. The present study also

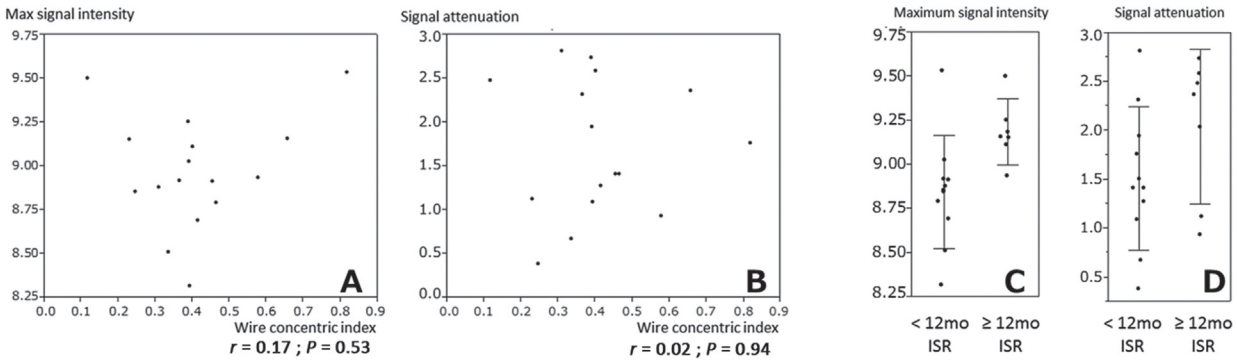

Figure 2. Lesion-level analysis. **A:** Correlation between maximum signal intensity and wire concentric index (WCI). **B:** Correlation between signal attenuation and WCI. **C:** Comparison of maximum signal intensity in mid-term and late in-stent restenotic lesions. **D:** Comparison of signal attenuation in mid-term and late in-stent restenotic lesions. ISR indicates in-stent restenosis. Bars: standard error.

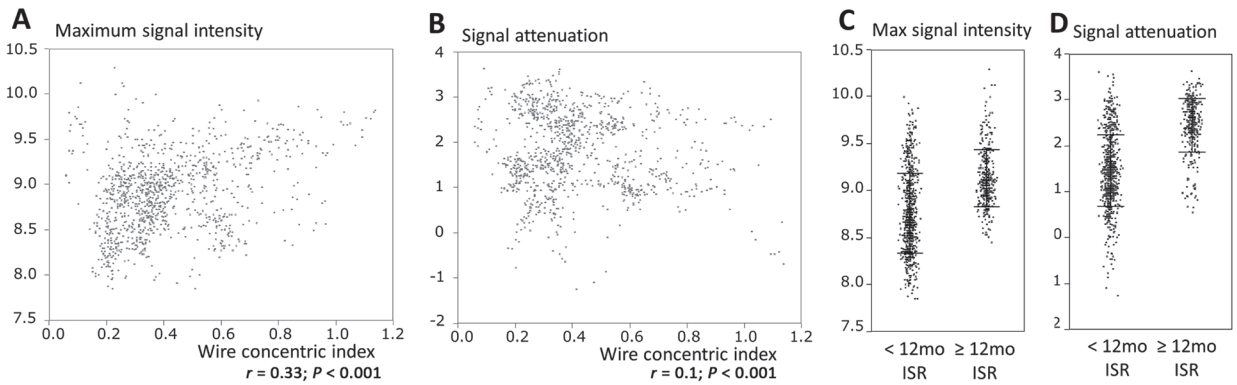

Figure 3. Frame-level analysis. **A:** Correlation between maximum signal intensity and wire concentric index (WCI). **B:** Correlation between signal attenuation and WCI. **C:** Differences in maximum signal intensity between mid-term and late in-stent restenotic lesions. **D:** Differences in signal attenuation between mid-term and late in-stent restenotic lesions. ISR indicates in-stent restenosis. Bars: standard error.

showed that higher maximum signal intensity was observed in late in-stent restenotic lesions. This result is consistent with other previous studies which visualized cholesterol crystal clefts and macrophages by showing high-intensity signals in OCT images.[12,16,17] The quantified data in the present study supports the assertion that *in vivo* neoatherosclerosis can be identified using OCT > 1 year after stent implantation.

Kang, *et al* also showed that neoatherosclerosis tends to appear earlier after DES implantation than after implantation of bare metal stents.[10] However, we could not compare the difference between DES and bare metal stents because of the small sample size in the present study. Further validation should be performed using pathologic materials from a cohort with a larger number of cases.

This study also demonstrated the utility of contemporary quantitative tissue characterization. To date, intravascular ultrasound has been commonly used to quantify atherosclerotic tissue[18] and neointimal proliferation after DES implantation.[19] Despite the excellent spatial resolution and image quality of coronary OCT,[4,20,21] a gold standard method for signal quantification has yet to be established.[22] Minimal beam reflection and refraction are required in OCT imaging for accurate and detailed signal quantification.[22,23] Beam direction has a significant influence on image quality in coronary OCT.[22,23] This study is the first to utilize semiautomated quantified image analysis data in the evaluation of in-stent restenotic lesions. In performing dedicated OCT tissue property analysis, image position must be recognized as a potential source of bias.[22,23]

The present study also achieved good interobserver and intraobserver variability in quantitative OCT image analysis in cases of in-stent restenosis. It is already widely known that OCT has much better spatial resolution than intravascular ultrasound.[13] Nevertheless, automated tissue property OCT analysis which makes the most of great spatial resolution has yet to be demonstrated. A previous investigation has shown a relationship between plaque embolism and myocardial damage following a poor prognosis.[24] If the quantitative automatic evaluation of atherosclerosis using OCT is reliable, it should facilitate better interventional strategies for individual patients.

This study had several limitations. First, it was based on a retrospective analysis with a limited sample size. Second, quantitative OCT analysis has not been validated by histology for the identification of neoatherscrelosis. Third, no data from another intra-coronary imaging modality other than OCT were presented.

Conclusion: OCT demonstrated stronger signal attenuation and higher maximum signal intensity in late in-stent restenotic lesions, indicating the possibility of neoatherosclerosis. Further

investigations on the application of tissue property OCT analysis to coronary interventional remedies are warranted.

REFERENCES

1. Moses JW, Leon MB, Popma JJ, *et al*. Sirolimus-eluting stents versus standard stents in patients with stenosis in a native coronary artery. N Engl J Med 2003; 349: 1315-23.
2. Park DW, Hong MK, Mintz GS, *et al*. Two-year follow-up of the quantitative angiographic and volumetric intravascular ultrasound analysis after nonpolymeric paclitaxel-eluting stent implantation: late "catch-up" phenomenon from ASPECT Study. J Am Coll Cardiol 2006; 48: 2432-9.
3. Suzuki N, Angiolillo DJ, Monteiro C, *et al*. Variable histological and ultrasonic characteristics of restenosis after drug-eluting stents. Int J Cardiol 2008; 130: 444-8.
4. Suzuki N, Coletta J, Guagliumi G, Costa MA. Clinical applications of OCT. In: Lemos PA, Schoenhagen P, Lansky AJ, ed. *Diagnostic Methods in the Cardiac Catheterization Laboratory: A Practical Approach for Special Clinical Situations.* 1st ed. London: Informa Healthcare, 2009: 146-57.
5. Guagliumi G, Costa MA, Sirbu V, *et al*. Strut coverage and late malapposition with paclitaxel-eluting stents compared with bare metal stents in acute myocardial infarction: optical coherence tomography substudy of the Harmonizing Outcomes with Revascularization and Stents in Acute Myocardial Infarction (HORIZONS-AMI) Trial. Circulation 2011; 123: 274-81.
6. Suzuki N, Kozuma K, Isshiki T. Role of microvessels in occlusive in-stent restenosis. Rev Esp Cardiol 2012; 65: 376. (English, Spanish)
7. Kim JS, Fan C, Choi D, *et al*. Different patterns of neointimal coverage between acute coronary syndrome and stable angina after various types of drug-eluting stents implantation; 9-month follow-up optical coherence tomography study. Int J Cardiol 2011; 146: 341-6.
8. Suzuki N, Kozuma K, Kyono H, *et al*. Predominant microvessel proliferation in coronary stent restenotic tissue in patients with diabetes: insights from optical coherence tomography image analysis. Int J Cardiol 2013; 168: 843-7.
9. Suzuki N, Kozuma K, Maeno Y, *et al*. Quantitative coronary optical coherence tomography image analysis for the signal attenuation observed in-stent restenotic tissue. Int J Cardiol 2010; 145: 392-4.
10. Kang SJ, Mintz GS, Akasaka T, *et al*. Optical coherence tomographic analysis of in-stent neoatherosclerosis after drug-eluting stent implantation. Circulation 2011; 123: 2954-63.
11. Coletta J, Suzuki N, Nascimento BR, *et al*. Use of optical coherence tomography for accurate characterization of atherosclerosis. Arq Bras Cardiol 2010; 94: 250-4, 268-72, 254-9. (Review) (English, Potuguese, Spanish)
12. Tearney GJ, Yabushita H, Houser SL, *et al*. Quantification of macrophage content in atherosclerotic plaques by optical coherence tomography. Circulation 2003; 107: 113-9.
13. Bezerra HG, Costa MA, Guagliumi G, Rollins AM, Simon DI. Intracoronary optical coherence tomography: a comprehensive review clinical and research applications. JACC Cardiovasc Interv 2009; 2: 1035-46. (Review)
14. Guagliumi G, Musumeci G, Sirbu V, *et al*. Optical coherence tomography assessment of in vivo vascular response after implantation of overlapping bare-metal and drug-eluting stents. JACC Cardiovasc Interv 2010; 3: 531-9.
15. Xu C, Schmitt JM, Carlier SG, Virmani R. Characterization of atherosclerosis plaques by measuring both backscattering and attenuation coefficients in optical coherence tomography. J Biomed Opt 2008; 13: 034003.
16. Tearney GJ, Waxman S, Shishkov M, *et al*. Three-dimensional coronary artery microscopy by intracoronary optical frequency domain imaging. JACC Cardiovasc Imaging 2008; 1: 752-61.
17. Tahara S, Morooka T, Wang Z, *et al*. Intravascular optical coherence tomography detection of atherosclerosis and inflammation in murine aorta. Arterioscler Thromb Vasc Biol 2012; 32: 1150-7.
18. Suzuki N, Costa MA. Intravascular ultrasound volumetric quantification: the current "gold standard" for characterization of coronary artery disease. Rev Esp Cardiol 2006; 59: 862-4. (Spanish)
19. Suzuki N, Nanda H, Angiolillo DJ, *et al*. Assessment of potential relationship between wall shear stress and arterial wall response after bare metal stent and sirolimus-eluting stent implantation in patients with diabetes mellitus. Int J Cardiovasc Imaging 2008; 24: 357-64.
20. Sato D, Koga S, Yasunaga T, *et al*. Culprit segments identified by optical coherence tomography in patients with acute myocardial infarction: two case reports. Cardiovasc Interv Ther 2012; 27: 47-51.
21. Inami S, Wang Z, Ming-juan Z, Takano M, Mizuno K. Current status of optical coherence tomography. Cardiovasc Interv Ther 2011; 26: 177-85.
22. Tearney GJ, Regar E, Akasaka T, *et al*. Consensus standards for acquisition, measurement, and reporting of intravascular optical coherence tomography studies: a report from the International Working Group for Intravascular Optical Coherence Tomography Standardization and Validation. J Am Coll Cardiol 2012; 59: 1058-72.
23. Suzuki N, Guagliumi G, Bezerra HG, *et al*. The impact of an eccentric intravascular ImageWire during coronary optical coherence tomography imaging. EuroIntervention 2011; 6: 963-9.
24. Reffelmann T, Hale SL, Dow JS, Kloner RA. No-reflow phenomenon persists long-term after ischemia/reperfusion in the rat and predicts infarct expansion. Circulation 2003; 108: 2911-7.